# Highly Oriented Growth of Catalytically Active Zeolite ZSM-5 Films with a Broad Range of Si/Al Ratios

*Donglong Fu, Joel E. Schmidt, Zoran Ristanović, Abhishek Dutta Chowdhury, Florian Meirer, and Bert M. Weckhuysen\**

*Abstract: Highly b-oriented zeolite ZSM-5 films are critical for applications in catalysis and separations and may serve as models to study diffusion and catalytic properties in single zeolite channels. However, the introduction of catalytically active $Al^{3+}$ usually disrupts the orientation of zeolite films. Herein, using structure-directing agents with hydroxy groups, we demonstrate a new method to prepare highly b-oriented zeolite ZSM-5 films with a broad range of Si/Al ratios (Si/Al = 45 to $\infty$). Fluorescence micro-(spectro)scopy was used to monitor misoriented microstructures, which are invisible to X-ray diffraction, and show $Al^{3+}$ framework incorporation and illustrate the differences between misoriented and b-oriented films. The methanol-to-hydrocarbons process was studied by operando UV/Vis diffuse reflectance micro-spectroscopy with on-line mass spectrometry, showing that the b-oriented zeolite ZSM-5 films are active and stable under realistic process conditions.*

**Z**eolites are crystalline aluminosilicate materials with angstrom-scale pores, and are industrially used at vast quantities owing to their robust stability under harsh conditions (e.g., fluid catalytic cracking and nuclear-waste treatment) as well as shape and size selectivity (e.g. alkylation reactions and the methanol-to-hydrocarbons (MTH) process).[1–4] One of the most important zeolites is ZSM-5 with the MFI framework, which is globally applied in enormous quantities in petroleum refining and bulk chemical manufacturing, driving continued research.[4,5] An innovative approach to enhance catalytic performance is to prepare homo-epitaxially grown zeolite ZSM-5 as continuous, oriented films with accessibility to only the straight zeolite channels. These film materials could serve as high-flux membranes with a combined reaction-separation functionality, wherein continuous size-selective product

removal would maximize conversion.[6–13] Moreover, the relative hydrophobicity/hydrophilicity of the films can be tuned by careful control of the Al content, forming a material capable of more diverse separations than those possible with the Al-free analogue.[14] Comparable to 2D zeolite nanosheets for surface chemistry studies,[15] uniform zeolite films are a promising model system for applying advanced characterization techniques (e.g. near-field optical techniques, such as tip-enhanced Raman (spectro)scopy (TERS), single-molecule fluorescence microscopy as well as grazing incidence characterization methods) to explore the synthesis mechanisms of both bulk and oriented-film zeolites, as well as to study 3D diffusion and related reactivity through a single pore orientation of zeolite ZSM-5 down to the level of a single molecule.[16]

Purely siliceous, highly *b*-oriented MFI films have been systematically researched in the past decades, and show ultra-selective, high-flux separation performance with enhanced diffusion properties due to the accessibility to only straight channels coupled with their hydrophobic nature.[17–19] However, the fabrication of highly *b*-oriented zeolite ZSM-5 films with Brønsted acid sites has rarely been reported,[20,21] and the framework introduction of $Al^{3+}$ into zeolite films is known to modify their growth, leading to highly overgrown materials when using tetrapropylammonium ($TPA^+$), the commercial structure-directing agent (SDA) for ZSM-5 synthesis.[22] The same phenomena has also been found with a SDA-free secondary growth media (SGM) synthesis.[23]

Herein we report a versatile second growth method to fabricate highly *b*-oriented zeolite ZSM-5 films with a broad range of Si/Al ratios by employing triethanolamine (TEOA) or inexpensive alcohols as the SDAs. These SDAs have hydroxy groups which chelate $Al^{3+}$,[24,25] allowing its slow release into the synthesis mixture, and avoiding the formation of misoriented micro-structures, which are demonstrated at the microscale using the highly sensitive technique of fluorescence micro-(spectro)scopy (FMS). To explore the range of Si/Al ratios across which $TPA^+$ can direct highly *b*-oriented zeolite ZSM-5 films, different Si/Al ratios (63, 125, and 250) in the SGM (solution 1 in Table S1 in the Supporting Information) were first prepared according to reported procedures.[17,18] Films with needle-like overgrowth were obtained in the SGM with a Si/Al ratio of 63 (Figure 1b) and 125 (Figure S1a) after a 15 h reaction. Decreasing to 8 h did not prevent the formation of these overgrowth structures (Figure S2c). Both samples (Si/Al = 63 (Figure 1e) and Si/Al = 125 (Figure S1c)) show three new XRD peaks that can be attributed to the (400), (600) and (800) directions, demonstrating the formation of misoriented structures in

[*] D. Fu, Dr. J. E. Schmidt, Dr. Z. Ristanović, Dr. A. D. Chowdhury,
Dr. F. Meirer, Prof. Dr. B. M. Weckhuysen
Inorganic Chemistry and Catalysis group
Debye Institute for Nanomaterials Science
Faculty of Science, Utrecht University
Universiteitsweg 99, 3584 CG Utrecht (The Netherlands)
E-mail: b.m.weckhuysen@uu.nl
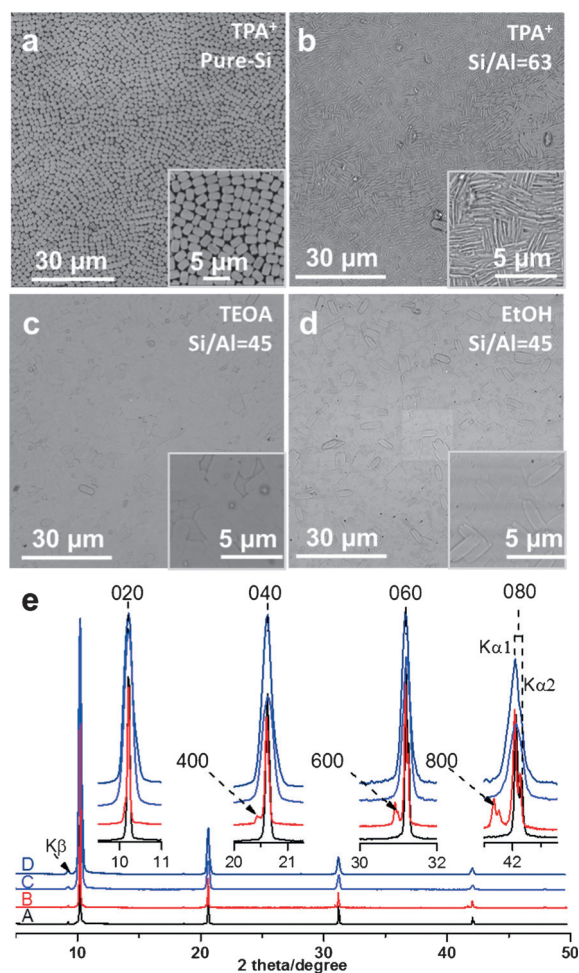Homepage: http://www.inorganic-chemistry-and-catalysis.eu

**Figure 1.** a)–d) Scanning electron microscopy (SEM) images of a) purely siliceous MFI monolayer and zeolite ZSM-5 films from the monolayer in a secondary growth media (SGM) with Si/Al = b) 63, c) 45, and d) 45, and different structure-directing agents (SDAs); e) traces (A), (B), (C), and (D) display representative X-ray diffraction (XRD) patterns of the samples in (a), (b), (c), and (d), respectively. Note that the SDAs used in the SGM solutions are b) tetrapropylammonium (TPA$^+$), c) triethanolamine (TEOA), and d) ethanol (EtOH), respectively.

the films.[17] Only when the Al content in the SGM was reduced to Si/Al = 250 could a highly *b*-oriented film be prepared as suggested by SEM and XRD (Figure S1b and S1c). The overgrowth in Al-containing TPA$^+$ systems can be attributed to the propensity of Al$^{3+}$ to favor nucleation over crystal growth, which does not occur in the pure-Si system.[26] Moreover, TPA$^+$ primarily helps to incorporate silicate species, leading to the known phenomenon of Al zoning in zeolite ZSM-5, resulting in the formation of crystallographic defects due to the Al-induced distortion of zeolite framework.[27] For comparison, an Al-free MFI film (Figure S3) was easily prepared under the same conditions, with preferential *b*-orientation and no overgrowth observed even after 42 h.

As it was not possible to prepare highly *b*-oriented zeolite ZSM-5 films with an Al content higher than Si/Al = 250 using TPA$^+$ as the SDA, we explored a strategy to intrinsically suppress nucleation—which is a potential cause of the

overgrowth due to the presence of Al$^{3+}$—by altering the SDA to properly incorporate Al$^{3+}$. Drawing on inspiration from past zeolite synthesis, triethanolamine (TEOA) was used to replace TPA$^+$ as the SDA for the synthesis of zeolite ZSM-5 films.[24, 28] It is known that Al$^{3+}$ can be chelated by TEOA, resulting in its slow release into reaction solution during synthesis, avoiding nucleation, which may prevent overgrowth.[24] As shown in Figure 1c, TEOA was able to direct the formation of a continuous and overgrowth-free zeolite ZSM-5 film from a SGM with Si/Al = 45 (solution 2), with preferential *b*-orientation (Figure 1e). To test if this result is due to the tertiary amine or the hydroxy groups, a TEOA-structure-like alcohol (see Section S3), 2-hydroxy-methyl-1,3-propanediol (HPD), was used as the SDA, and a highly *b*-oriented zeolite ZSM-5 film with Si/Al = 45 (Figure S4) was obtained. This illustrates that hydroxy groups are the key to the homo-epitaxial growth of the highly *b*-oriented zeolite ZSM-5 films, and not the amine. Furthermore, environmentally friendly ethanol (EtOH) was employed as the SDA,[29,30] and a continuous (Figure 1d) and overgrowth-free highly *b*-oriented (Figure 1e) zeolite ZSM-5 film with Si/Al = 45 was also obtained. As the results from SEM and XRD suggest, continuous, *b*-oriented films from Si/Al = 45 to ∞ could be obtained with both TEOA and EtOH as the SDAs (Figure S5). Further investigations into the importance of hydroxy groups were conducted (Figure S6) and it was determined that they were the key to suppressing overgrowth. A series of organics with different numbers of hydroxy groups, namely 1OH (methanol, 2-propanol, and t-butanol) and 2OH (ethylene glycol, 1,6-hexanediol) and 4OH (penta-erythritol), as the SDAs in the SGM with Si/Al = 45 were tested to determine the generality of this approach. SEM (Figure 2) and XRD (Figure S7) suggest that continuous, *b*-oriented zeolite ZSM-5 films could be prepared by all above SDAs, except penta-erythritol (Figure 2 f). It is possible that its four hydroxy groups interact too strongly with Al species, interrupting the crystallization of ZSM-5. Thus, hydroxy groups alone can suppress the overgrowth.
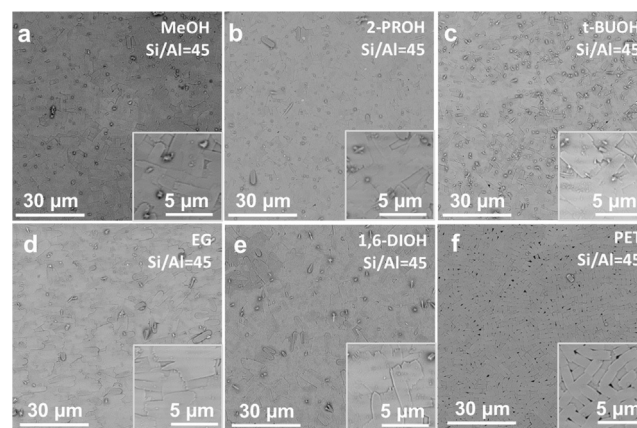


**Figure 2.** Scanning electron microscopy (SEM) images of zeolite ZSM-5 films from purely siliceous MFI monolayer in a secondary growth media (SGM) with Si/Al = 45 using a) methanol (MeOH), b) 2-propanol (2-PROH), c) t-butanol (t-BUOH), d) ethylene glycol (EG), e) 1,6-hexanediol (1,6-DIOH), and f) penta-erythritol (PET) as the structure-directing agents (SDAs), respectively.

While the structural features and orientation of zeolite ZSM-5 films could be characterized by SEM and XRD, it is difficult to decode the fabrication of the films and assert that the XRD perfect films are free from misoriented structures at the microscale owing to the inherent detection limitations of the technique. Moreover, the presence of a small amount of $Al^{3+}$ renders laboratory XRD unreliable to monitor its framework incorporation, since the unit cell volume increase from such a small amount of Al will be difficult to quantify. Therefore, FMS, with a high sensitivity to fluorescent product molecules from the Brønsted acid-catalyzed methoxystyrene oligomerization,[31] was employed to examine the quality of the films. Specifically, as shown in Figure 3, the resulting fluorescent products trapped in certain zeolite channels, with their fingerprint fluorescence emission bands, can be used as markers for assessing structural features, and the orientation as well as the framework incorporation of $Al^{3+}$ in zeolite films by using wide-field (WFM) and confocal (CFM) fluorescence micro-(spectro)scopy, respectively.[32–34] Using a highly *b*-oriented zeolite ZSM-5 monolayer and large zeolite ZSM-5 crystals, we determined the locations of the transition dipole moments of the products relative to the channel system (see Supporting Information). It was found that the trimeric carbocations (emission at ca. 650 nm with emission region of 640–680 nm) were confined with its dipole moment exclusively along the straight channels, while the linear dimeric carbocations (emission at ca. 600 nm with emission region of 580–620 nm) could be trapped with its dipole moment along

both channels.[31,34] Thus, the trimeric carbocation can be applied as a sensitive marker for the examination the film orientation since any misoriented zeolite domains will be fluorescent in the emission region of 640–680 nm in a horizontally positioned zeolite film (Figure 3e).

Under WFM, the TPA-directed zeolite ZSM-5 film prepared from the SGM solution with Si/Al = 63 in the horizontal position showed a large number of fluorescent, needle-like structures (Figure 3b), consistent with the SEM image (Figure 1b). Remarkably, TEOA- or EtOH-directed zeolite ZSM-5 films with a very high Al content (Si/Al = 45) clearly show honey-comb-like fluorescent features (Figure 3c,d), attributed to the catalytically active regions formed by laterally filling the inter-crystal spaces between the siliceous seed crystals with aluminosilicate zeolite material. This result shows the potential of applying WFM to probe the fabrication of zeolite films. The CFM study of the WFM fluorescent structures in the TPA-directed film showed the co-existence of strong emission regions of 580–620 nm and 640–680 nm (Figure 3f), demonstrating that these domains are misoriented (shown in Figure 3e). The fluorescence results (Figure S11) also illustrate that when using $TPA^+$ as the SDA, a highly *b*-oriented zeolite ZSM-5 film with only a tiny amount of Al (Si/Al = 250) can be obtained. However, as shown in Figure 3g,h, unlike the TPA-directed analogue, both the TEOA- and EtOH-directed zeolite ZSM-5 films in horizontal position showed only one emission region of 580–620 nm from the linear dimeric carbocations, and were
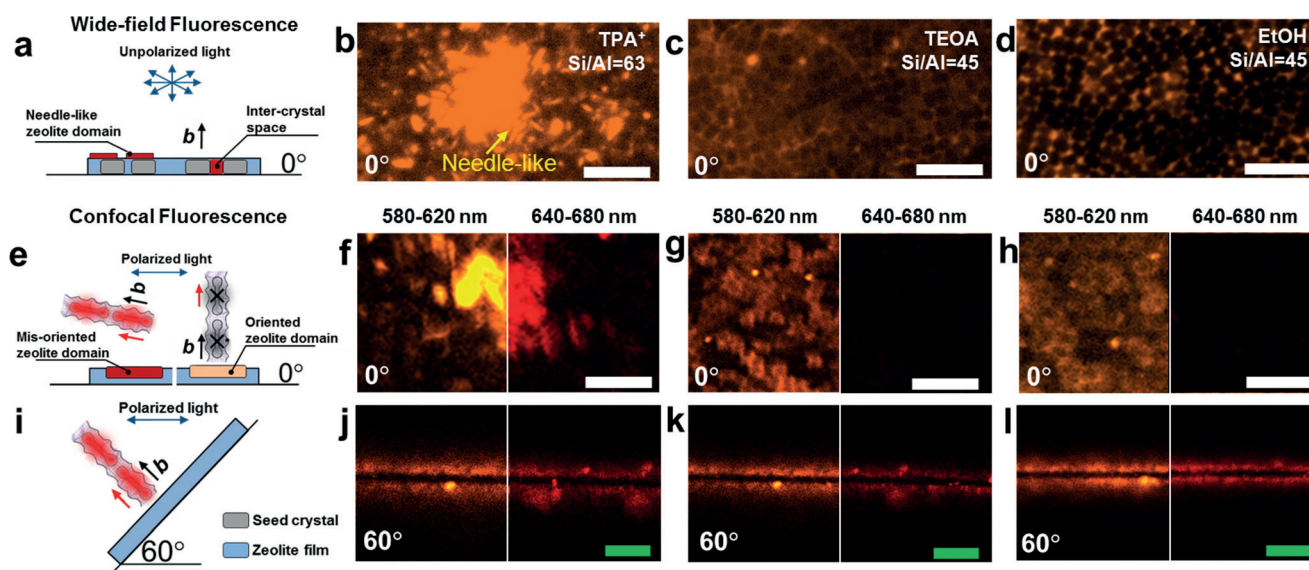


***Figure 3.*** a) Schematic representation of the wide-field fluorescence microscopic (WFM) study of a zeolite ZSM-5 film in its horizontal position (0°) with needle-like domains and inter-crystal spaces. b)–d) WFM images of the zeolite ZSM-5 films (0°) grown in a secondary growth media (SGM) with Si/Al = b) 63, c) 45, and d) 45, respectively, and different structure-directing agents (SDAs). e) Schematic representation of the confocal fluorescence micro-spectroscopic (CFM) study of a zeolite ZSM-5 film in its horizontal position (0°) with misoriented (left) and oriented (right) zeolite domains. Images f)–h) the corresponding CFM images from linear dimeric carbocation emission (580–620 nm) and trimeric carbocation emission (640–680 nm) in the same area of the zeolite films (0°). i) Schematic representation of the CFM study of a zeolite ZSM-5 film in its tilted position (60°) to confirm the trapped oligomerization products. Images j)–l) the corresponding CFM images from linear dimeric carbocation emission (580–620 nm) and trimeric carbocation emission (640–680 nm) of the 60° titled zeolite films. Note that the SDAs used in the SGM solutions are (b, f, and j) tetrapropylammonium ($TPA^+$), (c, g, and k) triethanolamine (TEOA), and (d, h, and l) ethanol (EtOH), respectively. The blue arrows denote polarized laser light and red arrows the transition dipole moment of the reaction products. White scale bar: 10 μm, green scale bar: 60 μm.

fluorescence-free in the trimeric region of 640–680 nm, demonstrating their perfect *b*-orientation. To confirm the confinement of the trimeric carbocation we have tilted all of the films by 60° (Figure 3i) so that the fluorescence of trimeric carbocation (if any is present) can be efficiently excited by the laser light. Two pronounced fluorescent lines, arising from the refraction of the laser on the film/substrate interface, with a CFM emission region of 640–680 nm,



*Figure 4.* a) Operando UV/Vis diffuse reflectance spectra of an ethanol-directed highly *b*-oriented zeolite ZSM-5 film with Si/Al = 45 in secondary growth media during the methanol-to-hydrocarbons (MTH) process at 673 K; b) The mass spectral profiles of dimethyl ether (DME), ethylene, and propylene as a function of time-on-stream (TOS).

were observed for all the films (Figure 3 j,k,l), consistent with the trimeric reaction product (Figure S8), and demonstrating the successful framework incorporation of $Al^{3+}$ and the perfect *b*-orientation of the films. A systematic 3D fluorescence study (Figure S12) with respect to the tilt angle of the EtOH-directed zeolite ZSM-5 film shows a gradual increase of the intensity ratio of about 650 nm to 600 nm with increasing tilt angle, demonstrating its perfect *b*-orientation. The successful framework incorporation of $Al^{3+}$ was further confirmed by removing the films from the substrates, and the fragments showed fluorescence (Figure S13) when randomly oriented. Moreover, the five zeolite films prepared with the range of alcohols were examined, and the fluorescence microscopy images and spectra (Figure S14) clearly show their perfect *b*-orientation and the presence of framework $Al^{3+}$. Additionally, further investigations (discussed in the caption of Figure S15) show that the FMS technique is highly sensitive to probe the film orientation and $Al^{3+}$ incorporation, and highlight the importance of applying a range of characterization techniques to verify film quality, as any single technique may not be sufficiently sensitive or accessible.

To demonstrate the utility of the highly *b*-oriented zeolite ZSM-5 films under realistic reaction conditions and provide secondary confirmation of their Brønsted acidity, *operando* UV/Vis diffuse-reflectance micro-spectroscopy with on-line mass spectrometry (MS) was utilized on an EtOH-directed, highly *b*-oriented zeolite ZSM-5 film with Si/Al = 45 during the MTH process conducted at 673 K.[35] The absorption maxima that developed with time-on-stream at around 410, 520, and 620 nm were assigned to neutral methylated benzenes, dienylic carbocationic/methylbenzenium ions, trienylic and methylated poly-arenium ions, respectively (Figure 4a and S16).[35,36] The clearly separated bands, compared to the broad signal normally found from bulk crystals,[36] can be used to easily explore the evolution of the reaction intermediates, and their contribution to the activity and deactivation of the MTH process demonstrates that the oriented films are promising for use as a model system to study catalytic reactions. Moreover, the on-line MS data reveals the existence of dimethyl ether (DME) and ethylene, along with propylene, as the reaction products during the
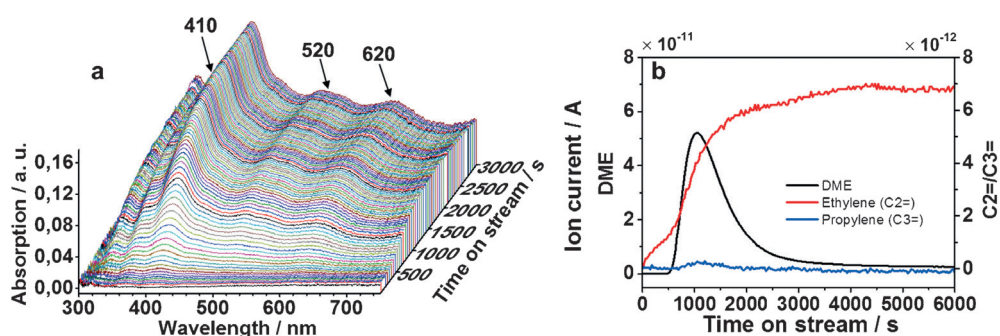
MTH process (Figure 4b and Figure S17), meaning that the films are catalytically active through their Brønsted acid sites.[37,38]

Summarizing, highly *b*-oriented zeolite ZSM-5 films with a broad range of Al contents have been fabricated using SDAs with hydroxy groups, which serve to suppress film overgrowth by properly introducing $Al^{3+}$ into the zeolite framework. The preparation route suggests that large-scale film production could meet scalability as well as strict health, safety and environmental requirements at an affordable cost, especially using EtOH. Moreover, the films prepared using this method were free of misoriented micro-structures and contain accessible Brønsted acid sites, showing not only potential for various catalytic applications, but that they can also serve as important model systems for understanding the synthesis mechanism of zeolite films, as well as catalysis in well-oriented zeolite channels.

### Acknowledgements

### Conflict of interest

The authors declare no conflict of interest.

[1] E. T. C. Vogt, G. T. Whiting, A. Dutta Chowdhury, B. M. Weckhuysen, *Adv. Catal.* **2015**, *58*, 143.

[2] J. Čejka, A. Corma, S. Zones, *Zeolites and Catalysis: Synthesis Reactions and Applications*, Wiley-VCH, Weinheim, **2010**.

[3] G. Ertl, H. Knözinger, F. Schüth, J. Weitkamp, *Handbook of Heterogeneous Catalysis*, 2nd ed., Wiley-VCH, Weinheim, **2008**.

[4] W. Vermeiren, J.-P. Gilson, *Top. Catal.* **2009**, *52*, 1131.

[5] S. K. Brand, J. E. Schmidt, M. W. Deem, F. Daeyaert, Y. Ma, O. Terasaki, M. Orazov, M. E. Davis, *Proc. Natl. Acad. Sci. USA* **2017**, *114*, 5101.

[6] T. Masuda, T. Asanuma, M. Shouji, S. R. Mukai, M. Kawase, K. Hashimoto, *Chem. Eng. Sci.* **2003**, *58*, 649.

[7] S. Haag, M. Hanebuth, G. T. P. Mabande, A. Avhale, W. Schwieger, R. Dittmeyer, *Microporous Mesoporous Mater.* **2006**, *96*, 168.

[8] O. Öhrman, J. Hedlund, V. Msimang, K. Möller, *Microporous Mesoporous Mater.* **2005**, *78*, 199.

[9] Z. Wang, Y. Yan in *Zeolites in Sustainable Chemistry* (Eds.: F.-S. Xiao, X. Meng), Springer, Berlin, **2016**, pp. 435–472.

[10] C. M. Lew, R. Cai, Y. Yan, *Acc. Chem. Res.* **2010**, *43*, 210.

[11] C. Zhou, N. Wang, Y. Qian, X. Liu, J. Caro, A. Huang, *Angew. Chem. Int. Ed.* **2016**, *55*, 12678; *Angew. Chem.* **2016**, *128*, 12869.

[12] Z. Cao, H. Jiang, H. Luo, S. Baumann, W. A. Meulenberg, J. Assmann, L. Mleczko, Y. Liu, J. Caro, *Angew. Chem. Int. Ed.* **2013**, *52*, 13794; *Angew. Chem.* **2013**, *125*, 14039.

[13] T. Yu, W. Chu, R. Cai, Y. Liu, W. Yang, *Angew. Chem. Int. Ed.* **2015**, *54*, 13032; *Angew. Chem.* **2015**, *127*, 13224.

[14] M. Lassinantti, F. Jareman, J. Hedlund, D. Creaser, J. Sterte, *Catal. Today* **2001**, *67*, 109.

[15] J. D. Kestell, J.-Q. Zhong, M. Shete, I. Waluyo, J. T. Sadowski, D. J. Stacchiola, M. Tsapatsis, J. A. Boscoboinik, *Catal. Today* **2017**, *280 Part 2*, 283.

[16] K. Varoon, X. Zhang, B. Elyassi, D. D. Brewer, M. Gettel, S. Kumar, J. A. Lee, S. Maheshwari, A. Mittal, C.-Y. Sung, et al., *Science* **2011**, *334*, 72.

[17] T. C. T. Pham, H. S. Kim, K. B. Yoon, *Science* **2011**, *334*, 1533.

[18] X. Lu, Y. Peng, Z. Wang, Y. Yan, *Chem. Commun.* **2015**, *51*, 11076.

[19] M. Y. Jeon, D. Kim, P. Kumar, P. S. Lee, N. Rangnekar, P. Bai, M. Shete, B. Elyassi, H. S. Lee, K. Narasimharao, et al., *Nature* **2017**, *543*, 690.

[20] T. Kita, S. Nishimoto, M. Matsuda, M. Miyake, *J. Am. Ceram. Soc.* **2009**, *92*, 3074.

[21] M. Grahn, A. Lobanova, A. Holmgren, J. Hedlund, *Chem. Mater.* **2008**, *20*, 6270.

[22] H. Liu, G. Liu, X. Zhang, D. Zhao, L. Wang, *Microporous Mesoporous Mater.* **2017**, *244*, 164.

[23] S. Mintova, J. Hedlund, V. Valtchev, B. J. Schoeman, J. Sterte, *J. Mater. Chem.* **1998**, *8*, 2217.

[24] G. Scott, R. W. Thompson, A. G. Dixon, A. Sacco, *Zeolites* **1990**, *10*, 44.

[25] R. Althoff, B. Schulz-Dobrick, F. Schüth, K. Unger, *Microporous Mater.* **1993**, *1*, 207.

[26] S. L. Burkett, M. E. Davis, *Chem. Mater.* **1995**, *7*, 1453.

[27] K. Ding, A. Corma, J. A. Maciá-Agulló, J. G. Hu, S. Krämer, P. C. Stair, G. D. Stucky, *J. Am. Chem. Soc.* **2015**, *137*, 11238.

[28] F. Gatti, E. Moretti, M. Padovan, M. Solari, V. Zamboni, *Zeolites* **1986**, *6*, 312.

[29] S. Sang, F. Chang, Z. Liu, C. He, Y. He, L. Xu, *Catal. Today* **2004**, *93–95*, 729.

[30] E. Costa, M. A. Uguina, A. de Lucas, J. Blanes, *J. Catal.* **1987**, *107*, 317.

[31] Z. Ristanović, A. V. Kubarev, J. Hofkens, M. B. J. Roeffaers, B. M. Weckhuysen, *J. Am. Chem. Soc.* **2016**, *138*, 13586.

[32] E. Stavitski, M. H. F. Kox, B. M. Weckhuysen, *Chem. Eur. J.* **2007**, *13*, 7057.

[33] C. Sprung, B. M. Weckhuysen, *J. Am. Chem. Soc.* **2015**, *137*, 1916.

[34] M. H. F. Kox, E. Stavitski, B. M. Weckhuysen, *Angew. Chem. Int. Ed.* **2007**, *46*, 3652; *Angew. Chem.* **2007**, *119*, 3726.

[35] A. D. Chowdhury, K. Houben, G. T. Whiting, M. Mokhtar, A. M. Asiri, S. A. Al-Thabaiti, S. N. Basahel, M. Baldus, B. M. Weckhuysen, *Angew. Chem. Int. Ed.* **2016**, *55*, 15840; *Angew. Chem.* **2016**, *128*, 16072.

[36] D. Mores, J. Kornatowski, U. Olsbye, B. M. Weckhuysen, *Chem. Eur. J.* **2011**, *17*, 2874.

[37] Y. Liu, S. Müller, D. Berger, J. Jelic, K. Reuter, M. Tonigold, M. Sanchez-Sanchez, J. A. Lercher, *Angew. Chem. Int. Ed.* **2016**, *55*, 5723; *Angew. Chem.* **2016**, *128*, 5817.

[38] A. Hwang, M. Kumar, J. D. Rimer, A. Bhan, *J. Catal.* **2017**, *346*, 154.